The Journal of Experimental Biology 215, 227-238

doi:10.1242/jeb.062836

RESEARCH ARTICLE

Functional properties and cell type specific distribution of I_h channels in leech neurons

Ednan Gerard[1], Peter Hochstrate[1], Paul-Wilhelm Dierkes[2] and Philippe Coulon[3,*]

[1]Institut für Neurobiologie, Heinrich-Heine-Universität, 40225 Düsseldorf, Germany, [2]Abteilung für Didaktik der Biowissenschaften, Johann Wolfgang Goethe-Universität, Sophienstraße 1-3, 60487 Frankfurt/Main, Germany and [3]Institut für Physiologie I, Westfälische Wilhelms-Universität, Robert-Koch-Str. 27a, 48149 Münster, Germany

*Author for correspondence (coulon@uni-muenster.de)

Accepted 9 October 2011

SUMMARY

The hyperpolarisation-activated cation current (I_h) has been described in many vertebrate and invertebrate species and cell types. In neurons, I_h is involved in rhythmogenesis, membrane potential stabilisation and many other functions. In this work, we investigate the distribution and functional properties of I_h in identified leech neurons of intact segmental ganglia. We found I_h in the mechanosensory touch (T), pressure (P) and noxious (N) neurons, as well as in Retzius neurons. The current displayed its largest amplitude in P neurons and we investigated its biophysical and pharmacological properties in these cells. I_h was half-maximally activated at –65 mV and fully activated at –100 mV. The current mutually depended on both Na^+ and K^+ with a permeability ratio p_{Na}/p_K of ~0.21. The reversal potential was approximately –35 mV. The time course of activation could be approximated by a single time constant of ~370 ms at –60 mV, but required two time constants at –80 mV of ~80 and ~560 ms. The current was half-maximally blocked by 0.3 mmol l^{-1} Cs^+ but was insensitive to the bradycardic agent ZD7288. The physiological function of this channel could be a subtle alteration of the firing behaviour of mechanosensory neurons as well as a stabilisation of the resting membrane potential.

Key words: leech, P neuron, I_h channel, caesium pharmacology, ZD7288.

INTRODUCTION

The hyperpolarisation-activated cation current (I_h) is involved in a range of functions of cells across species (Biel et al., 2009; Pape, 1996). In neurons, the current allows the control of rhythmic activity [e.g. in the thalamocortical system (McCormick and Pape, 1990b)], plays a key role in determining and stabilising the resting membrane potential (E_m) (Ludwig et al., 2003; Meuth et al., 2006; Pape, 1996) and has a wide range of other functions in processes such as dendritic integration, synaptic plasticity, synaptic transmission and the temporal processing of visual signals in the retina (for a review, see Biel et al., 2009). The current has several characteristic properties: (1) it is carried by both Na^+ and K^+ and has a reversal potential (E_{rev}) of approximately –20 mV under physiological conditions, hence it is inwardly directed at rest, causing a membrane depolarisation upon activation; (2) it is activated by hyperpolarising voltage deflections negative to approximately –55 mV; (3) its activation is facilitated by cyclic adenosine monophosphate (cAMP); and (4) it is blocked by low concentrations of Cs^+ and by the bradycardic agent ZD7288.

The first systematic description of a hyperpolarisation-activated cation conductance in leech neurons by Arbas and Calabrese showed that the electrical properties of heart interneurons (HN cells) include a Cs^+-sensitive component that is vital for these cells' oscillatory behaviour (Arbas and Calabrese, 1987a; Arbas and Calabrese, 1987b). This component appeared as a slow partial repolarisation after hyperpolarising current injections ('voltage sag', see Fig. 1). Later, the underlying current was shown to have the typical properties of neuronal I_h found in mammals, in that it was fully activated near –70 to –80 mV, its activation kinetics were voltage dependent between –100 and –60 mV (with time constants of 700 ms and 2 s, respectively) and it was carried by both Na^+ and K^+ (Angstadt and Calabrese, 1989).

In leech HN cells, I_h helps to control heartbeat: a series of inhibitory postsynaptic potentials hyperpolarises the membrane and causes a slow activation of I_h, which, in turn, mediates the depolarising phase (Angstadt and Calabrese, 1989). This function is similar to that in the thalamic neurons of mammals. Here, the current can provide pacemaker depolarisations after the preceding activity of hyperpolarising currents, which then trigger depolarisation-activated conductances such as low-threshold Ca^{2+} channels (Akasu et al., 1993; McCormick and Pape, 1990a; McCormick and Pape, 1990b; Pape and McCormick, 1989). Another function is to stabilise neurons near their E_m by lowering the input resistance upon hyperpolarising stimuli, causing both reduced amplitude of postsynaptic potentials ('shunting inhibition') and a return to more positive potentials. I_h was reported to play a role in stabilising the resting membrane potential in thalamic relay neurons, nodose sensory neurons and hippocampal interneurons (Doan and Kunze, 1999; Lupica et al., 2001; Meuth et al., 2006). Such a role has yet to be described for leech neurons, and a detailed analysis of I_h across leech neurons is not yet available.

Besides HN cells, a significant I_h that activates near –70 mV was also found in cultured leech Retzius neurons (Angstadt, 1999). In Retzius neurons of intact ganglia, voltage sags appeared to be substantially smaller, but I_h was nevertheless thought to be involved in the control of spontaneous action potential activity (Angstadt,

1999; Coulon et al., 2008). Marked voltage sags have been described in pressure (P) neurons *in situ* (Jansen and Nicholls, 1973; Klees et al., 2005), but the underlying mechanism has not been investigated. I_h was also found in salivary glands of the giant Amazon leech, *Haementeria ghilianii* (Wuttke and Berry, 1992).

The aims of this study were to: (1) determine which neurons show I_h or the characteristic voltage sag; (2) characterise key properties such as activation kinetics, voltage dependence, effects of impermeable cations, pharmacological profile and ion fluxes that constitute the current; and (3) elucidate the possible functional role this current plays in leech P neurons by assessing the excitability and the effects on the time course of AP firing.

We found that I_h preferentially appears in leech mechanosensory neurons and is largest in P neurons. We concentrated on P neurons for the biophysical and pharmacological characterisation of the current properties and for a discussion of the current's functional role.

MATERIALS AND METHODS

Preparation

Preparation was done as described previously (Coulon et al., 2008). Leeches were purchased from a commercial supplier (Zaug GmbH, Biebertal, Germany), or taken from the laboratory's own breeding stock, and identified as *Hirudo verbana* Carena 1820 (Annelida, Hirudinea) (see Siddall et al., 2007). Intact segmental ganglia were continuously superfused at a rate of ~5 ml min^{-1}, exchanging the chamber volume (0.05 ml) approximately 100 times per minute.

Electrophysiological recordings

Neurons were impaled by two sharp electrolyte-filled microelectrodes for recording E_m and for current injection. The electrodes were pulled on a vertical puller (Narishige PE-2, London, UK) from borosilicate capillaries (outer/inner diameter: 1.5 mm/0.86 mm, 0.15 mm filament; GC 150F-15, Clark Electromedical Instruments, Pangbourne, UK) and filled with 0.5 mol l^{-1} K_2SO_4 and 5 mmol l^{-1} KCl. Electrode resistance was ~90 MΩ. Electrodes were connected to a custom-made two-electrode voltage-clamp amplifier (modified TEC-05L, NPI Instruments, Tamm, Germany). The bath was grounded *via* an agar bridge. The output signals were digitised by an A/D converter (custom built, Zentralwerkstatt Biologie, Heinrich-Heine-Universität Düsseldorf, Germany; or Digidata 1322A, Molecular Devices, Sunnyvale, CA, USA) and were saved and analysed on a computer running in-house acquisition software (Eberhard von Berg, Institut für Neurobiologie, Heinrich-Heine-Universität Düsseldorf) or pClamp (Molecular Devices). Sampling frequency was 1 kHz for slow signals or 10 kHz for fast signals. Stimulus parameters were programmed on a MAX 21 pulse generator (Zeitz Instruments, Augsburg, Germany). The experimental setup was shielded by a Faraday cage and dampened by shock absorbers. Recordings were performed at room temperature (21°C). Fast current oscillations lasting roughly 10 ms after holding potential deflections in the voltage-clamp mode are not shown in the current traces to improve clarity.

Identification of neurons

The 21 segmental ganglia contain ~400 neurons arranged in six packets. The neurons investigated in this work can be divided into neurosecretory (Retzius and Leydig), motor [annulus erector (AE) and anterior pagoda (AP)] and mechanosensory [touch (T), pressure (P) and noxious (N)]. When ganglia are fixed ventral side up, Retzius neurons are easily identifiable based on their large size (~80 µm diameter of the soma) and central position. In the adjacent, posterior-lateral packet there are two pairs of P neurons (P_1, P_2), which can be distinguished by their electrophysiological characteristics. Depolarising current injections evoke large-amplitude action potentials and hyperpolarising current injections evoke characteristic voltage sags (see Fig. 1). The two anterior-lateral packets contain N, T and AP neurons. N and AP neurons are similar in size to P neurons, but N neurons generate very large action potentials with a prominent afterhyperpolarisation immediately after microelectrode impalement. AP neurons show spontaneous action potentials with low amplitude (~10 mV) at a frequency of ~5 Hz and a characteristic 'pagoda' shape (Nicholls, 1987). T neurons are smaller in size and do not show spontaneous action potentials. AE neurons are situated adjacent to neuron 251 and generate spontaneous low-amplitude (~7 mV) action potentials at ~10 Hz. Leydig neurons are adjacent to P_2 neurons, smaller in size and fire spontaneously at less than 4 Hz (Arbas and Calabrese, 1990).

Bath solutions and drugs

The standard leech saline (SLS) used for bath perfusion had the following composition (in mmol l^{-1}): 85 NaCl, 4 KCl, 2 $CaCl_2$, 1 $MgCl_2$ and 10 HEPES. The pH was adjusted to 7.40 with 1 mol l^{-1} NaOH, which increased the Na^+ concentration by 4 mmol l^{-1}. The osmolality of the SLS was 190 mosmol kg^{-1} H_2O (Osmomat 030, Gonotec, Berlin, Germany). Na^+-free solution was prepared by substitution of Na^+ with *N*-methyl-D-glucammonium ($NMDG^+$, prepared from *N*-methyl-D-glucamine and HCl; Sigma-Aldrich, Munich, Germany). Because of differences in osmotic activity, 105 mmol l^{-1} NMDG-Cl was used to substitute 89 mmol l^{-1} NaCl. In solutions containing 89 mmol l^{-1} Li^+, Na^+ was omitted and the pH was adjusted using LiOH. Finally, in solutions with varying K^+ concentrations, K^+ was either removed, or added to the solution without osmotic compensation. Monovalent and polyvalent cations were added as chloride salts without osmotic compensation.

In most preparations, the activation curve of I_h can be shifted towards more positive potentials by elevations in the intracellular cAMP concentration (Pape, 1996), thus increasing active I_h under resting conditions. In order to determine whether leech I_h channels are also sensitive to cAMP, we used the membrane-permeable cAMP analogue dibutyryl-cAMP (dbcAMP). Similarly, we applied 3-isobutyl-1-methylxanthine (IBMX, Sigma-Aldrich) to inhibit phosphodiesterases and, thus, increase the intracellular cAMP concentration (Bobker and Williams, 1989). To directly block I_h, we used Cs^+ (CsCl, Sigma-Aldrich) or ZD7288 (4-ethylphenylamino-1,2-dimethyl-6-methylaminopyrimidinium chloride; Tocris, Bristol, UK). For experiments in the presence of ZD7288, the bath perfusion was stopped after adding ZD7288 to the SLS.

Calculation of ion selectivity and analysis of experimental data

I_h is carried by cation channels that are selective for Na^+ and K^+ (Ho et al., 1994). Determining E_{rev} for I_h allows the calculation of the permeability ratio (p_{Na}/p_K) by rearranging Goldman's equation (see Aidley, 1989):

$$\frac{p_{Na}}{p_K} = \frac{\left[K^+\right]_o - e^{\frac{zFE_{rev}}{RT}}\left[K^+\right]_i}{e^{\frac{zFE_{rev}}{RT}}\left[Na^+\right]_i - \left[Na^+\right]_o}, \quad (1)$$

where $[K^+]_o$ and $[Na^+]_o$ are the extracellular and $[K^+]_i$ and $[Na^+]_i$ the intracellular concentrations of K^+ and Na^+, respectively, z is the number of elementary charges transferred, R is the universal gas constant, T is the absolute temperature and E_{rev} is the reversal

potential. The conductance ratio (g_{Na}/g_K) can be calculated using the formalism from Hodgkin and Huxley (Hodgkin and Huxley, 1952) (see Aidley, 1989):

$$\frac{g_{Na}}{g_K} = \frac{\left(E_K - E_{rev}\right)}{\left(E_{rev} - E_{Na}\right)}, \quad (2)$$

where E_K and E_{Na} are the equilibrium potentials for K^+ and Na^+, respectively. At a given E_m, I_h can be calculated by (Aidley, 1989):

$$I_h = g_K(E_m - E_K) + g_{Na}(E_m - E_{Na}). \quad (3)$$

By combining Eqns 2 and 3, g_{Na} and g_K, as well as the currents carried by Na^+ and K^+, can be calculated. For the intracellular and extracellular concentrations of Na^+ and K^+, data obtained with ion-sensitive microelectrodes were used (see below); these data were also used to calculate the equilibrium potentials of Na^+ and K^+.

Experimental data was analysed and fitted using Origin Software (Microcal, Northampton, MA, USA). Boltzmann's equation was used to calculate the voltage sensitivity of I_h activation, Hill's equation was used to calculate the dose–response curve, and single or sums of e-functions were used to describe the activation and deactivation kinetics of the current.

RESULTS

Voltage sag in identified leech neurons

The injection of a negative current into Retzius neurons or into the mechanosensory T, P and N neurons induced a membrane hyperpolarisation that was maximal after approximately 50 ms, but subsequently became smaller. The E_m reached a less negative plateau a few hundred milliseconds later (Fig. 1). This voltage sag was virtually abolished after the addition of 1–5 mmol l^{-1} Cs^+ to the bath (see Fig. 11A), indicating that it was mediated by I_h channels. The amplitude of the voltage sag was determined as the depolarisation between the peak of the negative voltage deflection and the potential at the end of a given current injection (Table 1). A voltage sag was absent in Leydig, AE and AP neurons (see Fig. 1). The voltage sag was largest by far in P neurons (see Fig. 1, Table 1), prominent in N neurons and small in Retzius neurons, where a voltage sag was discernible in the majority of cells (five out of nine). The smallest voltage sag was observed in three out of four tested T neurons.

Table 1. Size of the voltage sag in touch (T), pressure (P), noxious (N) and Retzius neurons

Cell type	Sag amplitude (mV)	E_m@I_{CC} (mV)	I_{CC} (nA)	*N*
T	1.8±1.0	–100±21	–2	4
P	24.7±4.7	–105±6	–3	8
N	9.0±4.2	–107±17	–2	8
Retzius	2.1±1.9	–101±11	–6	9

The sag amplitude was measured using injection currents (I_{CC}) that hyperpolarised the cells to approximately –100 mV (E_m@I_{CC}, where E_m is membrane potential). Voltage sags were absent in Leydig, annulus erector (AE) and anterior pagoda (AP) neurons (see Fig. 1).

The functional properties of the I_h channels were investigated in more detail in P neurons, because, in these cells, the voltage sag was largest. Furthermore, P neurons are sufficiently large and robust to routinely and reliably allow the application of the two-electrode voltage-clamp technique.

I_h in leech P neurons

A typical voltage-clamp experiment showing the activation of I_h in a P neuron is presented in Fig. 2. Initially, the E_m of the cell was clamped to a reference potential of –50 mV, which was slightly more negative than the mean E_m of leech P neurons (–44.3±4.9 mV, *N*=67) (see Schlue and Deitmer, 1984). This required a holding current of –0.4±0.3 nA (*N*=40). Clamping the neuron to –80 mV induced an inward current ('1' in Fig. 2B), reflecting the net change in membrane currents through ion channels that were already active at –50 mV (instantaneous current, I_i). Subsequently, an additional current mediated by I_h channels developed, which was evident from its biophysical and pharmacological properties (see below). I_h was maximal after approximately 0.5 s and persisted throughout the hyperpolarising pulse, indicating that the channels did not inactivate. Provided that the I_i remained constant during the hyperpolarising pulse, the I_h that was activated when stepping from –50 to –80 mV was obtained by subtracting I_i from the current at the end of the

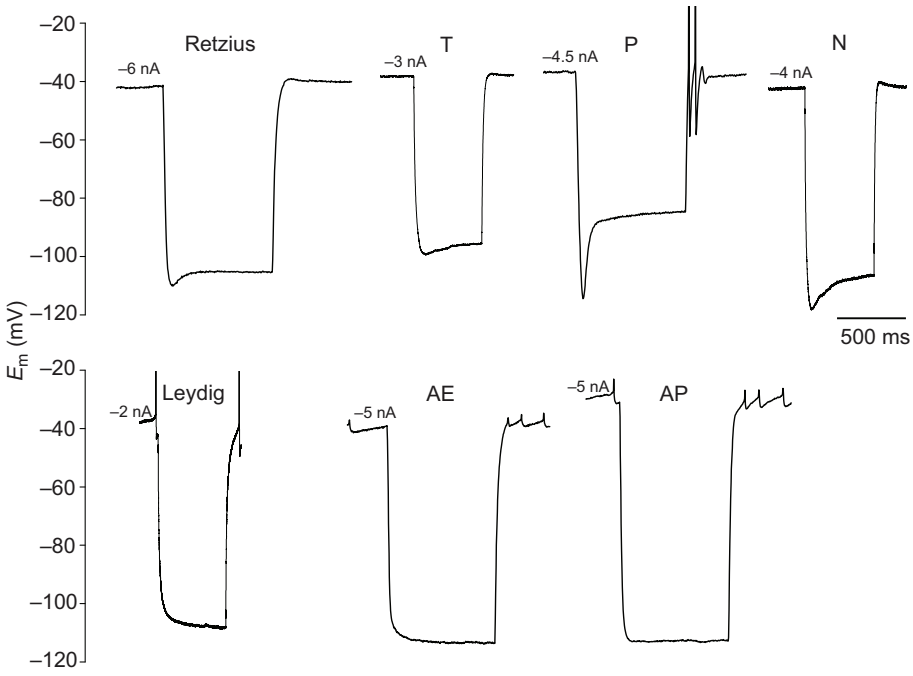

Fig. 1. Voltage sags in identified leech neurons. Upon injection of a hyperpolarising current of the given amplitude, Retzius neurons as well as the mechanosensory touch (T), pressure (P) and noxious (N) neurons showed voltage sags; i.e. after reaching a maximum hyperpolarisation, the membrane potential (E_m) repolarised partially. After cessation of the injection current, a transient depolarisation occurred, which in P neurons sometimes caused the generation of one or more action potentials. In Leydig, annulus erector (AE) and anterior pagoda (AP) neurons, voltage sags were not observed. The injection current (–2 to –6 nA for 500 or 800 ms) was adjusted such that the cells initially hyperpolarised to approximately –100 mV. Note the occurrence of spontaneous action potentials in Leydig, AE and AP neurons. The action potentials of P and Leydig neurons are truncated.

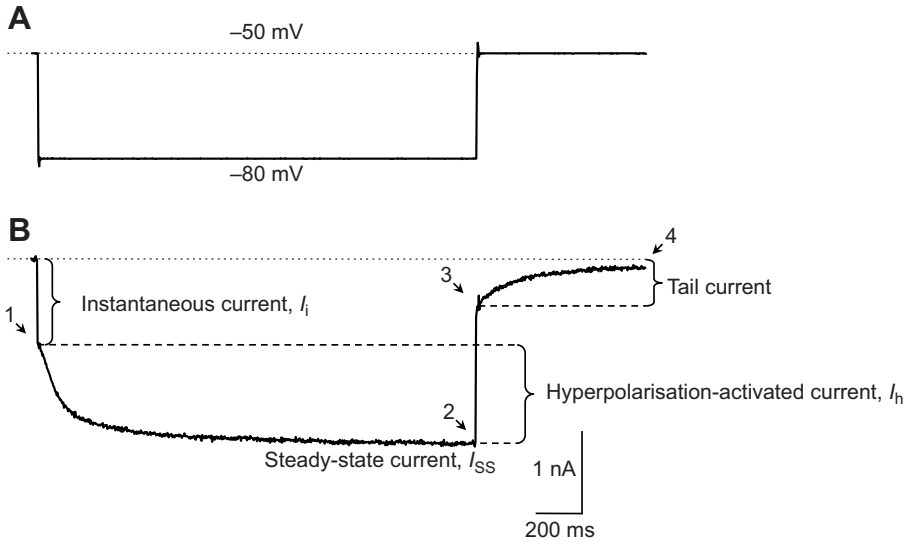

Fig. 2. Hyperpolarisation-activated cation (I_h) channels in a leech P neuron. Shifting E_m from the reference potential of –50 to –80 mV (A) induced the slow activation of a persistent inward current (B), which is mediated by I_h channels, as evident from the biophysical and pharmacological properties. The amplitude of I_h is given by the difference between the instantaneous current at the beginning of the voltage step (I_i; 1) and the membrane current at its end (steady-state or slow inward current, I_{SS}; 2). After return to the reference potential, a slowly falling tail current remained (3), which reflects the deactivation of the I_h channels. After complete deactivation, the current returned to resting values (4). The holding current at –50 mV was –0.4±0.3 nA (N=40).

pulse (steady-state or slow inward current, I_{SS}; '2' in Fig. 2B). After returning to –50 mV, an inwardly directed tail current ('3' in Fig. 2B) remained, which slowly declined as the I_h channels deactivated ('4' in Fig. 2B).

The activation of I_h was evident at E_m values slightly more negative than –50 mV (Fig. 3). With increasing hyperpolarisation, I_h became more and more prominent. At –80 mV, it was approximately as large as I_i (Fig. 3B, Fig. 4B). The tail current saturated with increasing, preceding hyperpolarisation, indicating that I_h channel activation was all but complete at approximately –80 mV (see Fig. 5).

The dependence of the I_i on the E_m was linear, the slope corresponding to an average input resistance of 23 MΩ (Fig. 3B, red line). In contrast, the membrane current at the end of the hyperpolarising pulse increased over-proportionally because of the increasing activation of I_h channels. At E_m values more negative than –70 mV, the slope of the current–voltage relationship appeared to approach a constant value, corresponding to an input resistance of 9 MΩ. At still more negative potentials the slope became smaller again, corresponding to an input resistance of 14 MΩ (see Fig. 8B, black squares).

Kinetics of activation and deactivation

The speed of I_h activation increased with growing membrane hyperpolarisation, as was previously described for other preparations (e.g. Budde et al., 2008) (see Fig. 3A). We approximated the activation kinetics by exponential functions as illustrated in Fig. 4, which shows the membrane currents induced by hyperpolarising the cell membrane to –60 or –80 mV. When the time course of I_h activation was fitted by a single exponential function, time constants

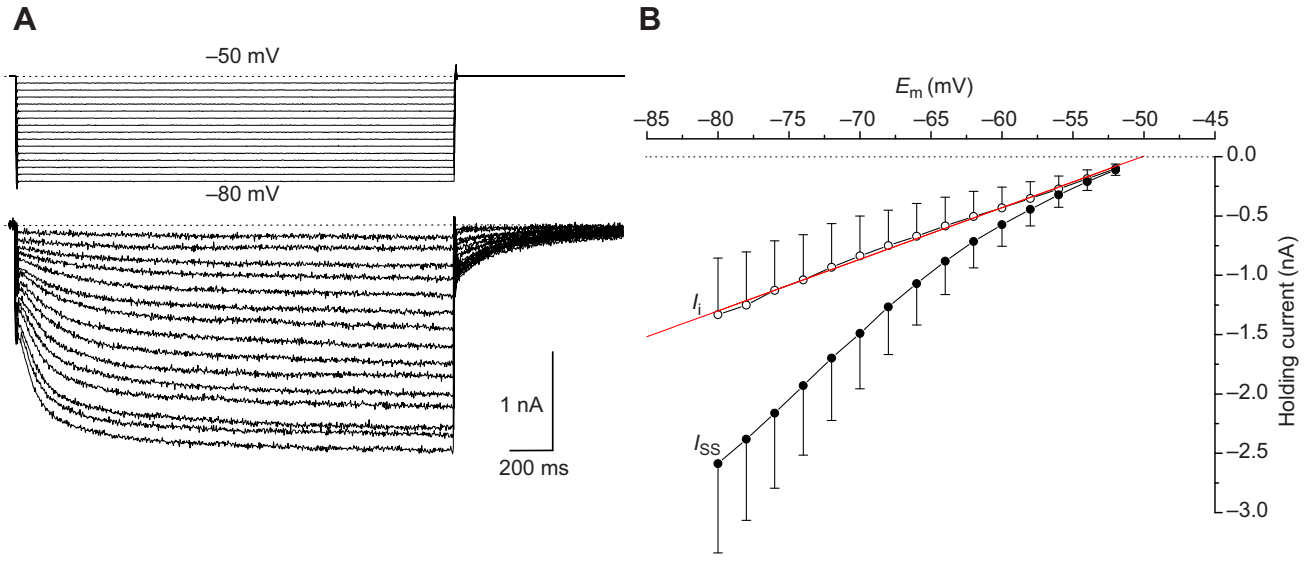

Fig. 3. Voltage dependence of I_i and I_{SS}. (A) Membrane currents upon shifting E_m from –50 to –80 mV (in 2 mV steps) for 2 s, recorded at intervals of 30 s. With increasing hyperpolarisation, the activation of I_h became progressively faster, while the decay of the tail current appeared to follow an invariant time course. (B) Relationship between membrane current and E_m, either at the beginning of the hyperpolarising step (I_i, open circles) or at its end, after activation of the I_h channels (I_{SS}, closed circles). Data points are means ± s.d. of 23 experiments. The voltage dependence of I_i was well fitted by a straight line (red line), the slope of which corresponded to an input resistance of 23 MΩ. In contrast, I_{SS} increased over-proportionally because of the increasing activation of the I_h channels. The difference between the two current–voltage relationships (I_{SS}–I_i) gives the amplitude of I_h activated by the respective voltage step.

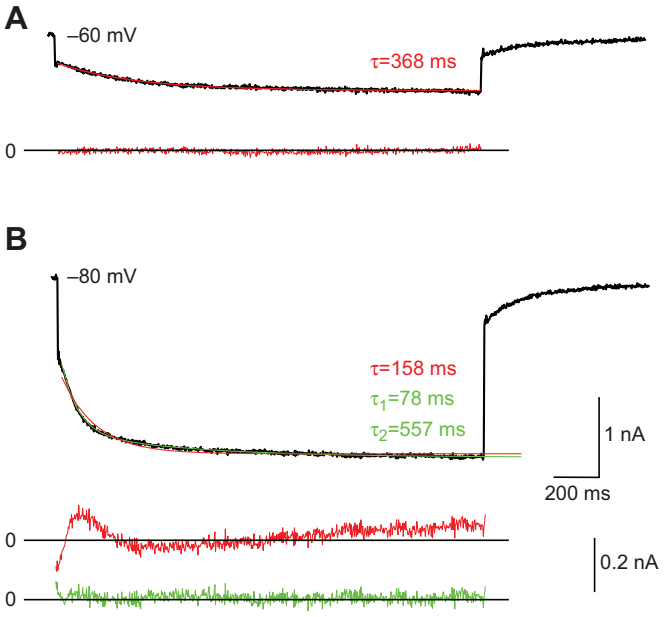

Fig. 4. Kinetics of I_h activation and deactivation. (A) At moderate hyperpolarisations (e.g. –60 mV), the activation of I_h was well fitted by a single exponential function. The upper trace shows the membrane current upon a hyperpolarisation from –50 to –60 mV (black trace), together with the approximation of I_h by a single exponential function with τ=368 ms and an amplitude of –0.38 nA (red curve). The lower trace shows the difference between recorded trace and calculated curve at an increased magnification, allowing an assessment of fit quality. See B for scale bars. (B) At stronger hyperpolarisations, the approximation of I_h by a single exponential function became progressively worse, but we obtained a satisfying fit using a sum of two exponential functions. The black trace shows the membrane current upon a hyperpolarisation to –80 mV, together with the approximation by a single exponential function (τ=158 ms; red curve) or the sum of two exponential functions (τ_1=78 ms, τ_2=557 ms; green curve). The fast component contributed –0.93 nA to the total current and the slow component contributed –0.33 nA. The lower two traces show the difference between the recorded trace and the curves calculated with one exponential function (red) or the sum of two exponential functions (green). The decline of the tail currents in A and B could be reasonably fitted by a single exponential function with a time constant of approximately 200 ms.

of 368±74 ms (for –60 mV) and 158±42 ms (for –80 mV) were obtained (N=12). At an E_m of –60 mV, the recorded trace and calculated curve corresponded very well to each other, but deviations were evident at –80 mV (see Fig. 4B, red trace). At this holding potential, a good fit was obtained by the sum of two exponential functions with time constants of 78±22 and 557±84 ms, whereby the fast component contributed approximately 75% to the total I_h. The decay of the tail current could be approximated by a single exponential function, with time constants ranging from 150 to 230 ms, and it was independent of the strength of the preceding hyperpolarisation (data not shown). In some recordings, the activation of I_h appeared to follow a slightly sigmoidal time course (see traces in Fig. 2B, Fig. 3A, Fig. 4B; see Discussion).

Voltage dependence of I_h channel activity

The tail current was recorded at constant electromotive forces, so that its amplitude should be proportional to the activity of the I_h channels at the end of the hyperpolarising pulse. The dependence of the tail current on the preceding E_m is shown in Fig. 5. An approximation of the experimental data by a Boltzmann function gave a half-maximal activation of the I_h channels at –65 mV.

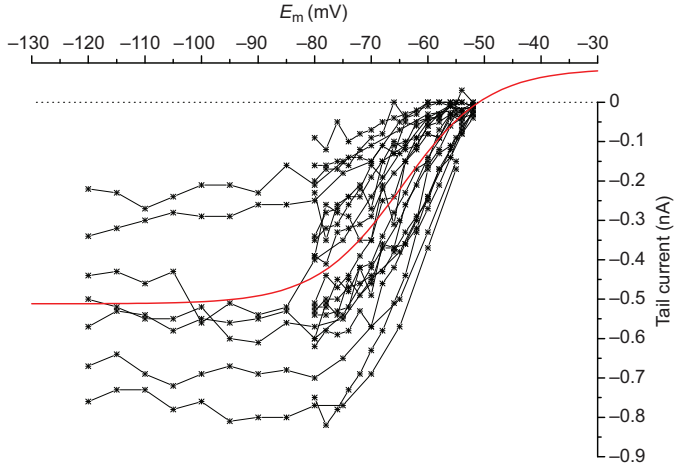

Fig. 5. Dependence of I_h channel activity on E_m. Relationship between the tail current recorded at –50 mV and E_m during the preceding hyperpolarisation. Data were obtained from 21 P neurons. In seven cells, E_m was shifted in 5 mV steps up to –120 mV and, in the remaining 14 cells, in 2 mV steps up to –80 mV (pulse duration 2 s, pulse interval 30 s). The continuous line represents an approximation of the data by a Boltzmann function, according to which the I_h channels are half-maximally activated at E_m=–65 mV.

According to this approximation, the activation of I_h channels started at –30 mV, and at –100 mV the channels were fully activated. The data in Fig. 5 also illustrate the large variability of the tail current in individual cells. Following hyperpolarisation to –80 mV, the tail current amplitudes ranged between –0.1 and –0.8 nA.

E_{rev} and ion permeability

The E_{rev} of I_h was determined by analysing the current flow through fully activated I_h channels at different E_m (Fig. 6A). For this purpose, E_m was shifted very briefly to a defined test potential and I_i at this potential was determined. Then, after a short pause, the cells were hyperpolarised to –100 mV for 3 s to achieve complete I_h channel activation. Finally, E_m was clamped again to the test potential. The membrane current measured at this time point is the sum of the I_i and the current mediated by the fully activated I_h channels. Its amplitude ideally depends on electromotive driving forces only.

The dependence of the maximal I_h on E_m is shown in Fig. 6B. Linear fits of the data gave a mean E_{rev} of –35±17 mV (N=7). Using this value and data on the intracellular and extracellular concentrations of Na^+ and K^+ previously obtained in our laboratory with ion-sensitive microelectrodes, p_{Na}/p_K was calculated to be 0.21. The calculation is based on the following values: $[K^+]_o$=5.8 mmol l^{-1} (at a bath concentration of 4 mmol l^{-1} K^+) (see Schlue and Deitmer, 1980), $[K^+]_i$=97 mmol l^{-1} (Schlue, 1991) (see also Klees et al., 2005; Schlue and Deitmer, 1984), $[Na^+]_o$=89 mmol l^{-1} (assumed to correspond to the Na^+ concentration of the bath solution) and $[Na^+]_i$=7.5 mmol l^{-1} (Hintz, 1999; Lucht, 1998) (see also Schlue, 1991). The equilibrium potentials were calculated to E_{Na}=+62 mV and E_K=–72 mV, and from the electromotive forces at E_{rev} we obtained a g_{Na}/g_K of 0.38. It could be argued that $[K^+]_o$ should be identical to the bath. In this case, p_{Na}/p_K would be 0.25 and g_{Na}/g_K would be 0.47. However, when the ganglion capsule was intact, the extracellular potassium concentration in the nerve cell body region was determined to be 5.8±0.6 mmol l^{-1} (mean ± s.d., N=27) (Schlue and Deitmer, 1980), whereas it was identical to the bath only after

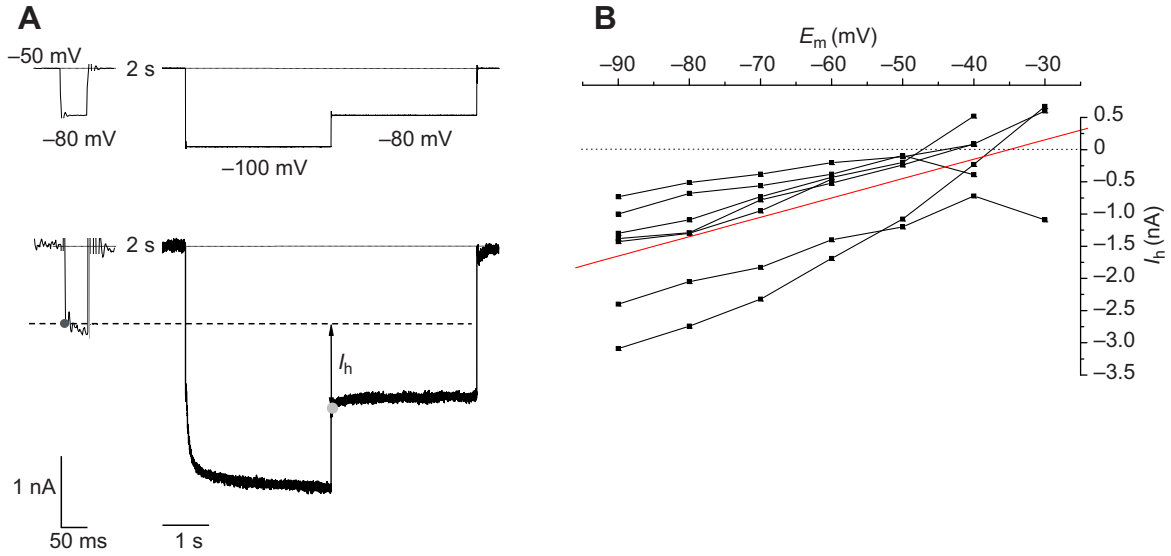

Fig. 6. Reversal potential of I_h. (A) Experimental protocol. To determine the instantaneous membrane current (I_i) at a given test potential (here, –80 mV), E_m was shifted correspondingly for 50 ms (upper trace). During this period, the membrane current increased slightly, probably because of the onset of I_h channel activation (lower trace). I_i was estimated by visual extrapolation of the recorded trace to the beginning of the voltage jump (dark grey circle). After a 2 s pause, E_m was shifted to –100 mV for 3 s to achieve full activation of the I_h channels. Subsequently, E_m was shifted back to the test potential, in order to determine the maximum I_h at this potential. For this, the previously recorded I_i was subtracted from the current recorded immediately after the potential jump from –100 mV to the test potential (light grey circle). This protocol was applied every 10 s at different test potentials to determine the membrane currents mediated by the fully activated I_h channels at –30 to –90 mV in 10 mV increments. (B) Current–voltage relationships. The data points represent the membrane currents mediated by the fully activated I_h channels at different E_m, as recorded from seven P neurons. In two cells, a reversal of I_h was not observed; in one cell I_h could only be measured between –90 and –60 mV. An error-weighted linear fit of the averaged data gave an E_{rev} of I_h of –35 mV (N=7, red line).

opening the ganglion capsule. Because the ganglion capsule was always intact in our experiments, we assumed $[K^+]_o$ was equal to 5.8 mmol l^{-1} for all subsequent calculations and discussions.

Block by external Cs^+ and insensitivity to ZD7288

A characteristic feature of I_h channels is the blockade by submillimolar concentrations of extracellular Cs^+ (DiFrancesco, 1982; Kaupp and Seifert, 2001; Pape, 1996). In P neurons, I_h was half-maximally blocked at a Cs^+ concentration of 0.3 mmol l^{-1}. At 5 mmol l^{-1} Cs^+, the block was virtually complete (Fig. 7). The onset of the block was fast and reversible within a few minutes. The time course of I_h activation was unaffected. The extracellular application of Ba^{2+}, Co^{2+} or Ni^{2+} (5 mmol l^{-1} each), or of the K^+ channel blocker tetraethylammonium (TEA, 20 mmol l^{-1}), for up to 10 min had no effect on I_h (data not shown).

The bradycardic agent ZD7288 selectively blocks I_h channels in a variety of vertebrate and invertebrate preparations. The half-maximal effect is mostly exerted at concentrations of 10 to

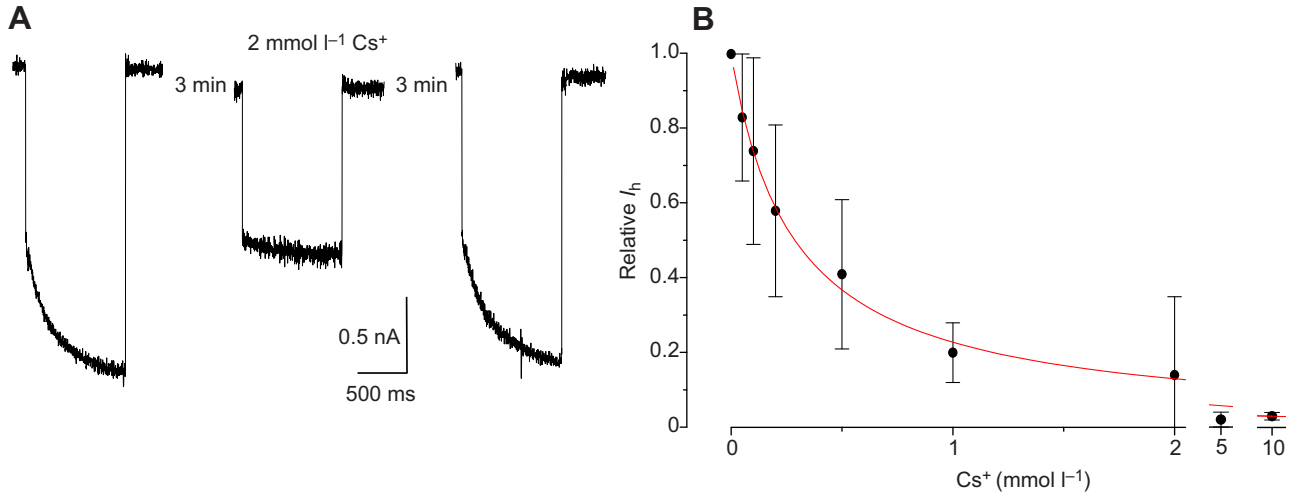

Fig. 7. I_h is blocked by Cs^+. (A) The presence of 2 mmol l^{-1} Cs^+ reversibly suppressed I_h. Traces show the membrane current upon shifting E_m from –50 to –80 mV for 1 s. Wash-in and wash-out time of Cs^+ was 3 min, as indicated. (B) I_h in solutions containing various Cs^+ concentrations were normalised to the mean current recorded before and after Cs^+ application. The approximation of the data by using the Hill formalism (red line) gave a half-maximal block of I_h at a Cs^+ concentration of 0.3 mmol l^{-1}. The Hill coefficient was 0.98. Data points are means ± s.d. of four to six experiments.

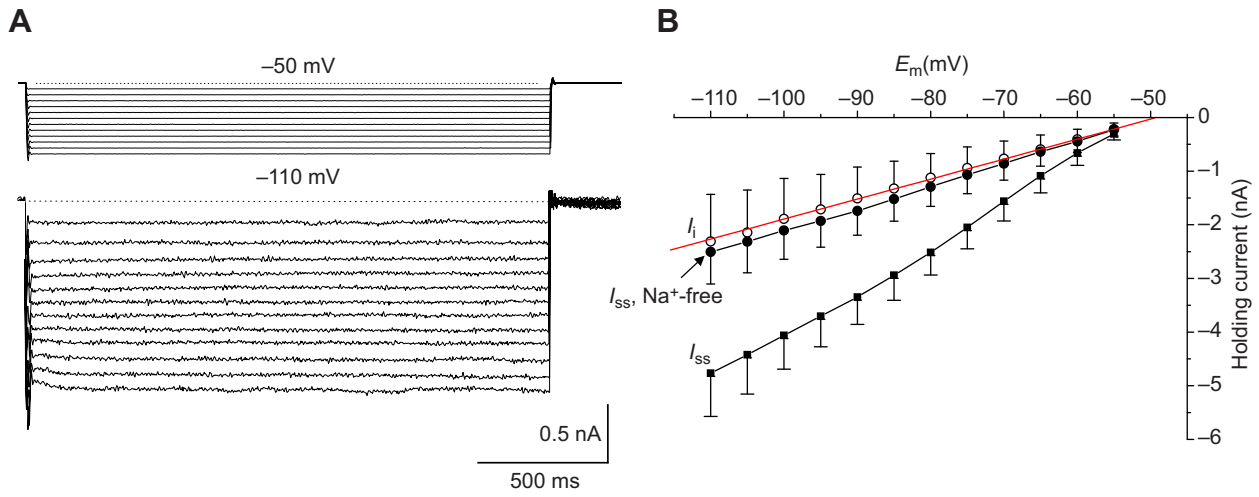

Fig. 8. I_h in Na^+-free solution. (A) Membrane currents upon shifting E_m from –50 to –110 mV (in 5 mV steps) for 2 s, recorded at intervals of 30 s. The recordings were started 3 min after replacing extracellular Na^+ by $NMDG^+$. In Na^+-free solution, I_h was virtually abolished. The holding current for clamping the cells to the reference potential was slightly reduced (–0.2±0.16 nA, N=7, cf. Fig. 2). (B) Relationship between the membrane current and E_m, either at the beginning of the hyperpolarising step (I_i; open circles) or at its end, after activation of the I_h channels (I_{SS}, Na^+-free; closed circles). Data points are means ± s.d. of five experiments. The voltage dependence of I_i was fitted by a straight line, the slope of which indicated an input resistance of 27 MΩ (see Fig. 3). For comparison, the I_{SS} recorded in SLS is also given (black squares; means ± s.d., N=7).

50 µmol l^{-1} (see Gasparini and DiFrancesco, 1997; Pirtle et al., 2010; Shin et al., 2001). In P neurons, however, even concentrations of 1–10 mmol l^{-1}, applied for up to 10 min, had no effect on I_h.

I_h in Na^+-free solution

After replacing extracellular Na^+ by $NMDG^+$, I_h was virtually abolished (Fig. 8). At –100 mV, the mean I_h amplitude was –0.2 nA, as compared with –2.2 nA in SLS (Fig. 8B). The tail current was inverted and strongly reduced, with maximum amplitudes of approximately ~0.1 nA (cf. Fig. 5); the time constant of deactivation varied between 250 and 400 ms. The voltage dependence of activation appeared to be unchanged: a Boltzmann approximation gave a half maximal activation at approximately –70 mV (data not shown). The effects of replacing extracellular Na^+ by $NMDG^+$ were fully reversible within a few minutes.

Replacing extracellular Na^+ by Li^+ also suppressed I_h and inverted the tail current (data not shown). The current for clamping the cells to –50 mV was increased (+1.3±0.6 nA, N=6). These effects occurred within 1 min after exchanging Na^+ for Li^+. Recovery was poor and, even 20 min after return to SLS, only a weak I_h was detectable. The tail current remained inverted and the current for clamping the cells to –50 mV often stayed increased.

Effect of extracellular K^+

After reducing the K^+ concentration of the bath solution, I_h and the tail current were strongly diminished (Fig. 9). Both currents were markedly increased when the extracellular K^+ concentration was raised. At low K^+ concentrations, E_{rev} of I_h was shifted towards more negative values, corresponding to the shift in the K^+ equilibrium potential. Under nominally K^+-free conditions, it was

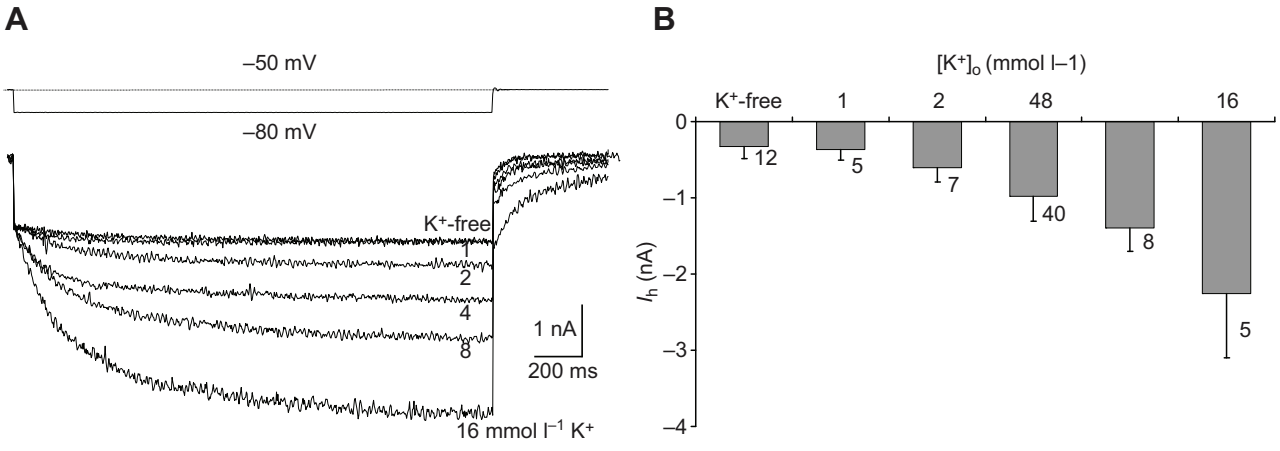

Fig. 9. Effect of extracellular K^+ on I_h. (A) Superimposed membrane currents upon shifting E_m from –50 to –80 mV for 2 s, recorded in the same P neuron 5 min after adjusting the K^+ concentration in the bath as indicated. For better comparison, the traces were slightly shifted vertically to bring the instantaneous currents recorded immediately after shifting E_m to congruence. (B) Amplitudes of I_h at –80 mV at different K^+ concentrations in the bath solution. Data are means ± s.d. of five to 40 experiments (N-values are shown to the right of the error bars).

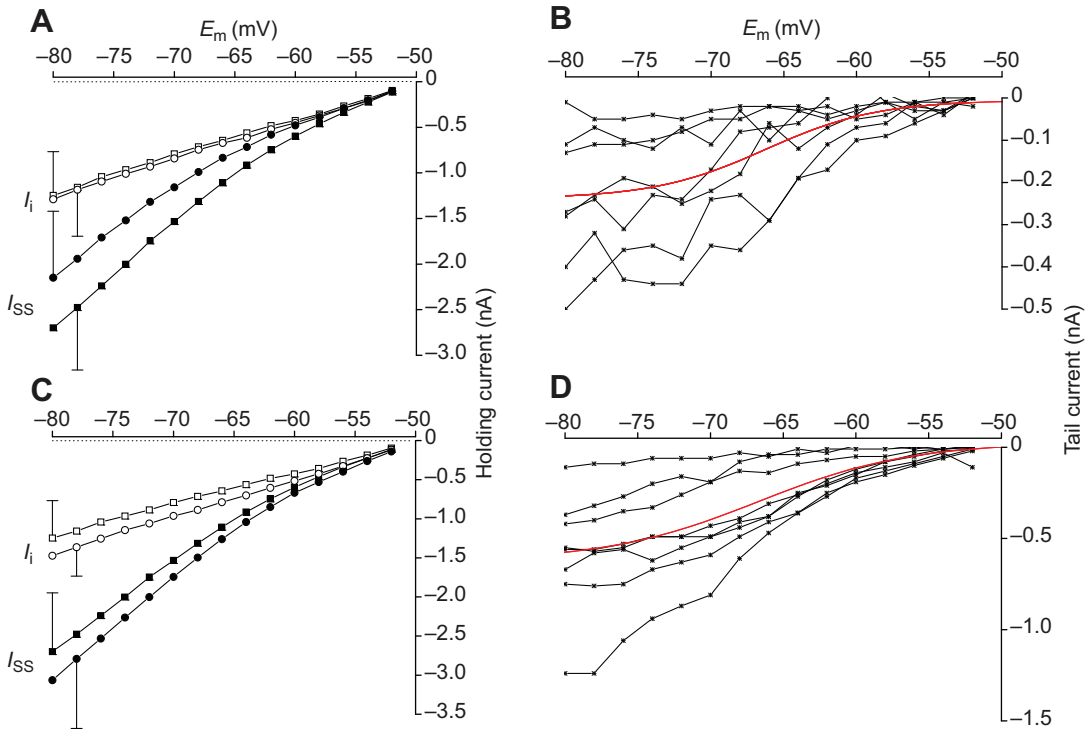

Fig. 10. Effect of cyclic nucleotides on I_h. (A,C) I_i (open symbols) and I_{SS} (closed symbols) in the presence (circles) and absence (squares) of dibutyryl-cAMP (dbcAMP, 1 mmol l^{-1}; A) or the phosphodiesterase blocker IBMX (1 mmol l^{-1}; C). For clarity, error bars are only shown exemplarily. Although I_h was decreased by ~50% in the presence of dbcAMP, the instantaneous current was unchanged. In IBMX, the amplitude of I_h remained unchanged but an overall decrease in the holding current was observed. (B,D) Relationship between tail currents at –50 mV and the preceding membrane hyperpolarisation, measured in the presence of dbcAMP (B) or IBMX (D). The recordings were started 10 min after adding dbcAMP or IBMX to the bath solution; single data points were measured at 10 s intervals. The continuous lines indicate approximations of the data by the Boltzmann equation, according to which the I_h channels were half-maximally activated at –66 mV (dbcAMP) or –67 mV (IBMX). Note that in the presence of IBMX, the maximum tail current was similar to that in SLS, whereas it was reduced by more than 50% in the presence of dbcAMP (cf. Fig. 5).

measured to be –63±23 mV (N=12). Surprisingly, the E_{rev} at increased bath K^+ concentrations were also found to be more negative than in SLS (8 mmol l^{-1} K^+: –40±5 mV, N=8; 16 mmol l^{-1}: –39±13 mV, N=5).

Effects of cAMP and IBMX

In most cells, cAMP shifts the voltage range of I_h channel activation to more positive values (see Kaupp and Seifert, 2001). In the presence of the membrane-permeable cAMP analogue, dbcAMP, or the phosphodiesterase inhibitor, IBMX (each 1 mmol l^{-1}), the I_h channels of leech P neurons were half-maximally activated at virtually the same E_m as in SLS (Fig. 10). Amplitudes of I_h and tail current were reduced by approximately 50% upon dbcAMP application, whereas they were unchanged in the presence of IBMX. The instantaneous current was almost unaffected by both dbcAMP and IBMX.

Effect of I_h on membrane excitability

The activation of I_h channels reduced the depolarising current necessary to elicit an action potential (Fig. 11A), suggesting an increased excitability. Furthermore, approximately 30% of the cells generated action potentials without the injection of a depolarising current upon repolarisation from hyperpolarised potentials (see Fig. 1). These effects cannot be attributed to accommodation, because a membrane hyperpolarisation in the presence of millimolar concentrations of Cs^+ never facilitated action-potential generation (Fig. 11A).

After activation of the I_h channels, the afterhyperpolarisation following an action potential shortened and subsequently reached a transient maximum (Fig. 11B, arrow). We never observed this when there was no preceding activation of the I_h channels. I_h channel activation did not affect amplitude and time course of the action potential. In the presence of Cs^+, amplitude, afterhyperpolarisation and latency (stimulus to peak) of the action potentials were reduced, whereas the time course remained unchanged (Fig. 11C).

I_h in other leech neurons

When using the voltage-clamp technique to assess I_h in AP, Leydig, N, T and Retzius neurons, I_h could be excluded in Leydig but not in AP neurons. The maximum I_h current varied from cell type to cell type and occurred at voltages between –80 and –120 mV (Table 2). As I_i may already contain I_h, we additionally determined the difference between the steady-state currents under control conditions (i.e. with activated I_h) and in the presence of 2 mmol l^{-1} Cs^+ (i.e. with I_h blocked; Cs^+-sensitive current, ΔI_{Cs}; Table 2). We found that the Cs^+-sensitive current was consistently larger than the I_h current as determined from the difference between I_{SS} and I_i. This corroborates that I_h is to some degree active at –50 mV, and/or that there is a rapidly activating I_h component, which is included in I_i, as has been reported previously (Budde et al., 2008; Mistrík et al., 2006; Proenza et al., 2002). When ΔI_{Cs} is set in relation to the total holding current at a given holding potential, thus giving an estimate of the contribution of I_h to the overall membrane conductance, it becomes apparent that the mechanosensory N and P neurons have

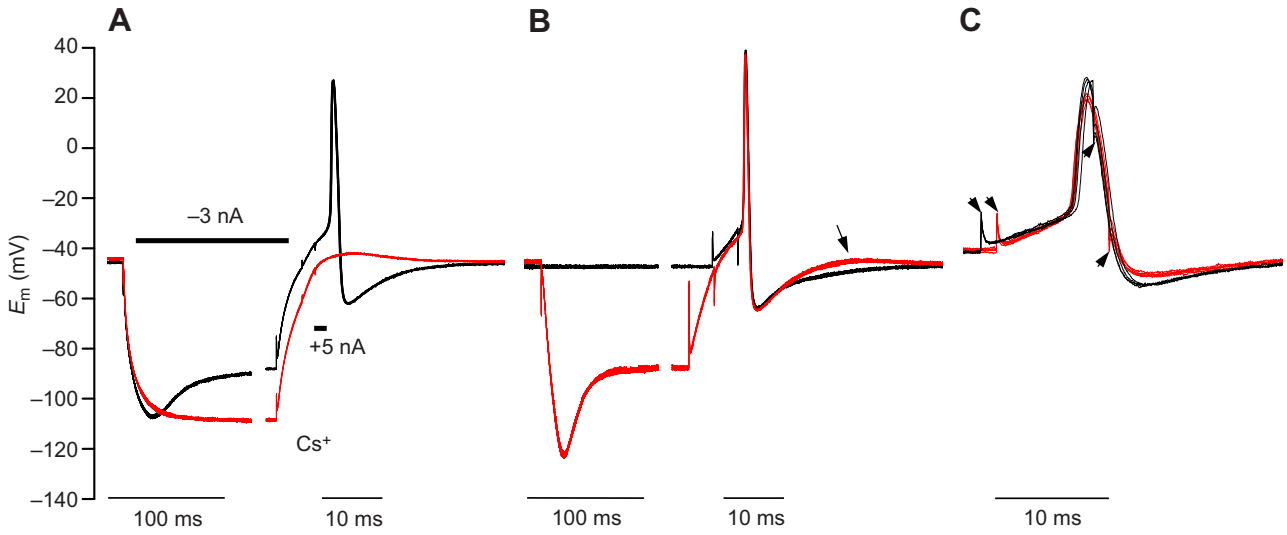

Fig. 11. Effect of I_h channel activation on membrane excitability and action potential waveform. (A) Membrane excitability. In this P neuron, action potentials could be reliably elicited by injecting a depolarising current of +5 nA for 5 ms, provided that the I_h channels had been activated by a preceding hyperpolarisation (–3 nA for 0.3 s; black trace). However, if the I_h channels were blocked by 1 mmol l^{-1} Cs^+, action potentials were never generated in response to this stimulus (red trace). Each trace represents the superimposition of five single recordings to demonstrate the reproducibility of the waveforms. The effect of Cs^+ was fully reversible within a few minutes. Identical results were obtained from five cells in total. (B) Action potential waveform. After activation of the I_h channels by a hyperpolarising current (–3 nA for 0.3 s), the afterhyperpolarisation following an action potential was shortened, and subsequently reached a transient maximum (red trace, arrow). This was never observed without preceding I_h channel activation (black trace). Amplitude and time course of the action potentials were not affected by I_h channel activation. As in A, each trace represents the superimposition of five single recordings. Traces were horizontally shifted to bring action potentials into congruence. In this P neuron, the injection of +2 nA for 5 ms was sufficient to reliably elicit an action potential, even without I_h channel activation. (C) Effect of Cs^+ on action potentials. Superimposed traces of five consecutively elicited action potentials under control conditions (black) and in the presence of 1 mmol l^{-1} Cs^+ (red). Traces were horizontally shifted to bring action potentials into congruence. Cs^+ reduced the peak amplitudes and the afterhyperpolarisation. Moreover, the latency from the beginning of the current injection (arrows mark the stimulus artefact, +2 nA for 10 ms) to the peak of the action potential was also reduced. The effect of Cs^+ was fully reversible. Similar results were obtained for five cells in total.

the largest I_h, followed by T, AP and Retzius neurons, whereas in Leydig neurons I_h appears to be virtually absent. We note that the values in Table 2 can only be a rough estimate, as Cs^+ may inhibit conductances other than I_h.

DISCUSSION

For leech HN cells, and briefly for Retzius and P neurons, I_h has been described before (Angstadt, 1999; Angstadt and Calabrese, 1989; Arbas and Calabrese, 1987b; Coulon et al., 2008; Klees et al., 2005). However, a detailed description of the distribution and biophysical properties of leech I_h across cell types was lacking. The findings presented here can be summarised as follows. First, voltage sags and the underlying I_h were observed in T, P, N and Retzius neurons. Second, the current was largest in P neurons. Third, the biophysical properties of the current largely matched those described in other preparations: (a) half-maximum activation occurred at –65 mV, complete activation at –100 mV; (b) the activation could be fitted by a single time constant of ~370 ms at –60 mV but required two time constants of ~80 and ~560 ms at –80 mV; (c) E_{rev} was determined to be –35±17 mV; and (d) the current mutually depended on both extracellular Na^+ and K^+, with a p_{Na}/p_K of 0.21. Fourth, half-maximal block of I_h was achieved at a Cs^+ concentration of 0.3 mmol l^{-1}. The current was insensitive to ZD7288. Fifth, after elevation of the intracellular cAMP concentration, I_h in leech P neurons showed a blockade, rather than a voltage shift of the activation curve. Sixth, the channels caused bursts of APs when a neuron was relieved from hyperpolarisation and modulated the form of afterhyperpolarisations. And finally, the function of I_h seems to include a subtle alteration of firing behaviour in leech mechanosensory neurons as well as a stabilising effect on E_m.

Activation kinetics

In some experiments, it was evident that I_h activation followed a sigmoidal time course (see Fig. 3A), as was found previously in leech heart interneurons [see fig. 2 in Angstadt and Calabrese (Angstadt and Calabrese, 1989)] and in most other systems (see Hestrin, 1987; Kaupp and Seifert, 2001). This phenomenon was interpreted as a delay-to-onset of the time-dependent component of I_h (Angstadt and Calabrese, 1989), i.e. the delay between the instantaneous component and the voltage-activated component of the membrane current. Unfortunately, in our experiments the early lag phase was

Table 2. Hyperpolarisation-activated cation currents (I_h) were observed in T, P, N, AP and Retzius neurons

Cell type	I_h (nA)	ΔI_{Cs} (nA)	$\%\Delta I_{Cs}$ of I_{SS}	*N*
AP	–0.1±0.2	–0.8±0.6	15±9	5
Leydig	+0.4±0.2	–0.2±0.8	0.2±27	5
N	–0.6±0.4	–0.9±1.0	39±29	8
P	–1.9±0.4	–2.8±1.4	47±24	7
T	–0.2±0.3	–0.4±0.3	16±9	4
Retzius	–0.4±0.4	–1.4±1.7	10±19	8

I_h was measured 500 ms after a voltage step from –50 mV to the holding potential that gave the largest I_h (see Fig. 2). When the current required for the voltage step in the presence of Cs^+ was deducted from the current measured under control conditions with active I_h (ΔI_{Cs}), the resulting values were always larger. The contribution of the current blocked by Cs^+ to the overall current required for the voltage step ($\%\Delta I_{Cs}$ of I_{SS}) reveals that N and P neurons have the largest relative I_h and will thus be influenced most by I_h activation. Because AE neurons are rather small and difficult to access using the two electrode current- and voltage-clamp techniques, AE neurons were not analysed (but see Fig. 1).

short and mostly hidden by the initial oscillations in the holding current. When the early lag was ignored, the activation of I_h could be well approximated by a single exponential function, if E_m was not too negative (Fig. 4A). At potentials that were more negative, a reasonable fit was only possible by applying a sum of two exponential functions (Fig. 4B). This biphasic activation has been reported previously (Budde et al., 1994; Pape, 1996) and was attributed to the existence of two distinct populations of I_h channels.

Ion selectivity

From the determined E_{rev} of I_h (–35±17 mV, N=7; Fig. 6), p_{Na}/p_K was calculated to be 0.21 by using the Goldman equation. This calculation was based on intracellular and extracellular concentrations of Na^+ and K^+ measured previously by ion-sensitive microelectrodes. g_{Na}/g_K was determined to be 0.38. Comparison with permeability and conductance ratios obtained from other preparations reveals that the values calculated here are within the same range [p_{Na}/p_K between 0.2 and 0.4 (for a review, see Pape, 1996); g_{Na}/g_K between 0.25 and 0.67 (e.g. Bolívar et al., 2008; Macri et al., 2002)].

At –80 mV, I_h was on average approximately –1.3 nA (see Figs 2, 3). With this value and the above conductance ratio, g_K is 21 nS and g_{Na} is 8 nS. These values, in turn, allow us to calculate the tail current when returning from –80 mV to –50 mV to –0.44 nA, which corresponds nicely with the experimental data (see Fig. 5).

The suppression of I_h after replacing Na^+ by Li^+ shows that the channels are virtually impermeable to Li^+, which is in accordance with previous findings (Biel et al., 2009; Pape, 1996; Wollmuth and Hille, 1992).

Pharmacological profile of I_h in leech neurons

One of the characteristics of I_h is its sensitivity to relatively low concentrations of Cs^+ [0.1–5 mmol l^{-1} (Pape, 1996)]. Cs^+ also blocks other voltage-dependent ion channels, such as delayed rectifier and inward rectifier K^+ channels, complicating its use as a sole criterion for the identification of I_h. In leech P neurons, I_h was insensitive to Ni^{2+}, Co^{2+} or Ba^{2+} (5 mmol l^{-1} each), as well as to TEA^+ (20 mmol l^{-1}; data not shown).

Another characteristic of I_h is its sensitivity to ZD7288. Leech P neurons were, however, completely insensitive to ZD7288 at concentrations as high as 10 mmol l^{-1}. Nevertheless, in our view, most other experimental data shown here strongly argue in favour of the assumption that leech I_h channels are very similar, albeit not identical, to classical, ZD7288-sensitive I_h channels found in other preparations. Although it is beyond the scope of this work to elucidate why ZD7288 does not block the channels, it is not uncommon that known and established selective blockers are ineffective in the leech preparation in known concentration ranges (e.g. Johansen and Kleinhaus, 1986). Moreover, an ineffective blockade of leech I_h by ZD7288 was reported previously for HN cells (Tobin and Calabrese, 2005).

Leech I_h channels also show unusual behaviour concerning their reactions to cAMP. I_h channels are often regulated by cAMP such that they shift their voltage dependency of activation towards more positive potentials, whereas kinetics and amplitudes remain largely unaltered (Kaupp and Seifert, 2001; Pape, 1996; Pape and McCormick, 1989). In leech P neurons, the membrane-permeable analogue dbcAMP did not change the voltage dependency of activation, but instead caused a 50% reduction of the current. Lack of regulation by cAMP has been reported before and has been attributed to both HCN1 and HCN3 subunits of the channel, with HCN3 even being slightly inhibited by cAMP (Biel et al., 2009). In some systems that selectively express HCN1, cAMP shifted the activation curve by only a few millivolts (Santoro et al., 1998) or not at all (Shin et al., 2001). The insensitivity of the voltage dependence of activation to cAMP points to the expression of the HCN1 and HCN3 subtypes in leech neurons. In support of HCN1 expression is the comparably fast activation kinetics (Shin et al., 2001). In support of HCN3 expression is the inhibition by cAMP.

Multi-ion pores

The dependence of I_h on the presence of extracellular Na^+ and K^+ suggests that the fluxes of Na^+ and K^+ through the I_h channels are dependent on one another. Thus, after replacing extracellular Na^+, I_h was all but absent. Under these conditions, a small Na^+ efflux can be expected. However, this was not taken into account for the calculations, as the intracellular Na^+ concentration drops in the absence of extracellular Na^+ to values of 1 mmol l^{-1} and lower (Hintz, 1999), so that a Na^+ efflux should be negligibly small. If, under these conditions, the K^+ component of the current persisted, an inward current of –0.59 nA would be expected at –100 mV (g_K=21 nS). However, the measured current was on average only –0.21 nA, indicating that g_K was reduced to roughly one-third of its original value in the absence of extracellular Na^+.

I_h was suppressed in the absence of K^+ in the bath solution (Fig. 9), arguing in favour of a mutual dependency of the two ions on one another within the channel pore. In a K^+-free bath solution, the extracellular K^+ concentration in the vicinity of the neurons' somata was measured to be 1.6±0.6 mmol l^{-1} (Schlue and Deitmer, 1980). Under K^+-free conditions, the lowest measured intracellular K^+ was 78 mmol l^{-1} (Schlue, 1991; Schlue and Deitmer, 1984) and intracellular Na^+ increased to ~20 mmol l^{-1} (Lucht, 1998). With these ion concentrations and assuming that extracellular Na^+ remains at 89 mmol l^{-1}, I_h can be calculated with the given g_K and g_{Na} to –0.56 nA at –80 mV. However, the measured current was only –0.33±0.16 nA (N=12; Fig. 9B), suggesting that g_{Na} was reduced by at least 40% in the K^+-free bath solution. This mutual dependency of ion conductances within a channel pore is a characteristic feature of multi-ion pores (Hestrin, 1987; Hille, 2001).

I_h or the lack thereof in other neurons of the leech

Leydig neurons fire spontaneously at low rates [<4 Hz (Arbas and Calabrese, 1990)] and were found to regulate heart rate in the leech. We show here that I_h is all but absent in Leydig neurons, so that the intrinsic rhythm observed in these neurons cannot be mediated by I_h. The only non-mechanosensory neurons showing considerable I_h were Retzius neurons. In these cells, the current may affect spontaneous action-potential generation (Angstadt, 1999) and does not seem to be involved in volume regulation (Coulon, 2005) (see Coulon et al., 2008). The voltage sag and I_h were smallest in T neurons, and it is questionable whether such a small current can have a functional relevance.

Physiological relevance

The nervous system of the medicinal leech is organised in ganglia that contain various neurons with well-known functions. This offers the opportunity to correlate physiological and functional aspects. The hyperpolarisation-activated inward current of leech HN cells was slightly different in its biophysical properties when compared with the I_h described here in leech P neurons. It began to activate near –50 mV, became fully activated between –70 and –80 mV, and had slow and voltage-dependent activation kinetics with single time constants ranging from 2 s at –60 mV to 700 ms at –100 mV. It had an E_{rev} of –21±5 mV and was blocked by 1–5 mmol l^{-1} extracellular

Cs^+ (Angstadt and Calabrese, 1989). HN cells interconnect by inhibitory chemical synapses, and their normal electrical activity consists of bursts of action potentials separated by periods of inhibition. The function of I_h in HN cells seems obvious: the cells hyperpolarise during the silent state so that I_h activates. This activation depolarises the membrane and helps the cells escape from the hyperpolarisation caused by inhibitory inputs. Accordingly, Cs^+ slows (Masino and Calabrese, 2002; Tobin and Calabrese, 2005) or even abolishes oscillatory behaviour (Angstadt and Calabrese, 1989).

The neurons described in this work displaying I_h were mostly mechanosensory and not spontaneously active. Thus, a pacemaker function of I_h like that described for HN cells can be excluded. Instead, two further functions may exist in leech P neurons: (1) a stabilising effect on E_m and (2) a subtle alteration of the firing behaviour. These neurons respond to mechanical stimuli of the skin with barrages of action potentials, proportional to the stimulus intensity, followed by a prominent hyperpolarisation that lasts for seconds or minutes and is caused by the activation of Ca^{2+}-activated K^+ channels and the activity of the Na^+/K^+-ATPase (Baylor and Nicholls, 1969; Jansen and Nicholls, 1973; Scuri et al., 2002). This hyperpolarisation will lead to the activation of I_h, which then helps to determine both the strength and duration of this hyperpolarisation. Moreover, a marked increase of the afterhyperpolarisation following each action potential is observed after prolonged sensory stimulation (Scuri et al., 2002). The afterhyperpolarisation is considered to have two major functions: it limits the firing frequency of the neuron and is responsible for generating spike-frequency adaptation. An activation of I_h should alleviate both effects, and indeed, we observed a shorter afterhyperpolarisation after I_h activation (Fig. 11B) as well as the occasional spontaneous generation of one or several action potentials upon repolarisation. Hyperpolarisations activate I_h, allowing counteracting depolarisations, so that the E_m is shifted back to its original value. *Vice versa*, depolarisations will cause deactivation of I_h, which would result in a counteracting hyperpolarisation. Additionally, after prolonged mechanosensory stimulation, and the subsequent strong hyperpolarisation, the activation of I_h could help to preserve the effect of mechanosensory inputs by increasing the excitability. Although this could be a common trait of mechanosensory neurons in the leech, it is unclear whether this is a necessity for somatosensory signalling (i.e. a mechanism to reduce spike-frequency adaptation) or an amplifying mechanism for post-stimulus intervals (providing increased sensitivity to stimuli). The idea of shunting inhibition by reducing the input resistance of P neurons is refuted somewhat by the fact that deactivation of I_h is slow: before it is complete, e.g. during depolarisation from a hyperpolarised E_m, I_h increases the neurons' excitability by a further depolarising tail potential. Additionally, it could be argued that increased excitability and shortened afterhyperpolarisation increase the neurons' firing rate, thereby possibly providing a more reliable sensory relay.

Although I_h is probably active near rest, the blockade with Cs^+ did not hyperpolarise E_m. This could be explained by an unspecific action of Cs^+. K^+ channels that may be active in leech P neurons could be blocked, e.g. the delayed rectifier and inward rectifier K^+ channels (Pape, 1996). This would mask the hyperpolarisation caused by blocking I_h with a depolarisation caused by blocking K^+ conductances. To what extent this occurs in leech P neurons is, however, unclear.

LIST OF SYMBOLS AND ABBREVIATIONS

AE	annulus erector (neuron)
AP	anterior pagoda (neuron)
cAMP	cyclic adenosine monophosphate
E_K	equilibrium potential for K^+
E_m	resting membrane potential
E_{Na}	equilibrium potential for Na^+
E_{rev}	reversal potential
g_{Na}/g_K	conductance ratio
HN	heart interneuron
IBMX	3-isobutyl-1-methylxanthine
I_h	hyperpolarisation-activated cation current
I_i	instantaneous current
I_{SS}	steady-state or slow inward current
N	noxious (neuron)
P	pressure (neuron)
p_{Na}/p_K	permeability ratio
R	universal gas constant
SLS	standard leech saline
T	touch (neuron)
T	absolute temperature
z	number of elementary charges transferred
ZD7288	4-ethylphenylamino-1,2-dimethyl-6-methylaminopyrimidinium chloride

ACKNOWLEDGEMENTS

The authors thank Claudia Roderigo and Simone Durry for excellent technical assistance and Prof. Dr Thomas Budde and Dr Susan Sangha for helpful comments on the manuscript.

FUNDING

This research received no specific grant from any funding agency in the public, commercial, or not-for-profit sectors.

REFERENCES

Aidley, D. J. (1989). *The Physiology of Excitable Cells*. Cambridge: Cambridge University Press.

Akasu, T., Shoji, S. and Hasuo, H. (1993). Inward rectifier and low-threshold calcium currents contribute to the spontaneous firing mechanism in neurons of the rat suprachiasmatic nucleus. *Pflügers Arch.* **425**, 109-116.

Angstadt, J. D. (1999). Persistent inward currents in cultured Retzius cells of the medicinal leech. *J. Comp. Physiol. A* **184**, 49-61.

Angstadt, J. D. and Calabrese, R. L. (1989). A hyperpolarization-activated inward current in heart interneurons of the medicinal leech. *J. Neurosci.* **9**, 2846-2857.

Arbas, E. A. and Calabrese, R. L. (1987a). Ionic conductances underlying the activity of interneurons that control heartbeat in the medicinal leech. *J. Neurosci.* **7**, 3945-3952.

Arbas, E. A. and Calabrese, R. L. (1987b). Slow oscillations of membrane potential in interneurons that control heartbeat in the medicinal leech. *J. Neurosci.* **7**, 3953-3960.

Arbas, E. A. and Calabrese, R. L. (1990). Leydig neuron activity modulates heartbeat in the medicinal leech. *J. Comp. Physiol. A* **167**, 665-671.

Baylor, D. A. and Nicholls, J. G. (1969). Chemical and electrical synaptic connexions between cutaneous mechanoreceptor neurones in the central nervous system of the leech. *J. Physiol.* **203**, 591-609.

Biel, M., Wahl-Schott, C., Michalakis, S. and Zong, X. (2009). Hyperpolarization-activated cation channels: from genes to function. *Physiol. Rev.* **89**, 847-885.

Bobker, D. H. and Williams, J. T. (1989). Serotonin augments the cationic current I_h in central neurons. *Neuron* **2**, 1535-1540.

Bolívar, J. J., Tapia, D., Arenas, G., Castanon-Arreola, M., Torres, H. and Galarraga, E. (2008). A hyperpolarization-activated, cyclic nucleotide-gated (I_h-like) cationic current and HCN gene expression in renal inner medullary collecting duct cells. *Am. J. Physiol.* **294**, C893-C906.

Budde, T., White, J. A. and Kay, A. R. (1994). Hyperpolarization-activated Na^+-K^+ current (I_h) in neocortical neurons is blocked by external proteolysis and internal TEA. *J. Neurophysiol.* **72**, 2737-2742.

Budde, T., Coulon, P., Pawlowski, M., Japes, A., Meuth, P., Meuth, S. G. and Pape, H. C. (2008). Reciprocal modulation of Ih and ITASK in thalamocortical relay neurons by halothane. *Pflügers Arch.* **456**, 1061-1073.

Coulon, P. (2005). Elektrophysiologie der Volumenregulation von Retzius-Neuronen im Zentralnervensystem des medizinischen Blutegels. PhD thesis, Heinrich-Heine-Universität, Düsseldorf, Germany.

Coulon, P., Wüsten, H. J., Hochstrate, P. and Dierkes, P. W. (2008). Swelling-activated chloride channels in leech Retzius neurons. *J. Exp. Biol.* **211**, 630-641.

DiFrancesco, D. (1982). Block and activation of the pace-maker channel in calf Purkinje fibres: effects of potassium, caesium and rubidium. *J. Physiol.* **329**, 485-507.

Doan, T. N. and Kunze, D. L. (1999). Contribution of the hyperpolarization-activated current to the resting membrane potential of rat nodose sensory neurons. *J. Physiol.* **514**, 125-138.

Gasparini, S. and DiFrancesco, D. (1997). Action of the hyperpolarization-activated current (I_h) blocker ZD 7288 in hippocampal CA1 neurons. *Pflügers Arch.* **435**, 99-106.

Hestrin, S. (1987). The properties and function of inward rectification in rod photoreceptors of the tiger salamander. *J. Physiol.* **390**, 319-333.

Hille, B. (2001). *Ion Channels of Excitable Membranes*. Sunderland, MA: Sinauer Associates.
Hintz, K. (1999). Elektrophysiologische charakterisierung der Mg^{2+}-regulation bei identifizierten neuronen und neuropil-gliazellen im zentralnervensystem des medizinischen blutegels. PhD thesis, Heinrich-Heine-Universität, Düsseldorf, Germany.
Ho, W. K., Brown, H. F. and Noble, D. (1994). High selectivity of the i(f) channel to Na+ and K+ in rabbit isolated sinoatrial node cells. *Pflügers Arch.* **426**, 68-74.
Hodgkin, A. L. and Huxley, A. F. (1952). A quantitative description of membrane current and its application to conduction and excitation of nerve. *J. Physiol.* **117**, 500-544.
Jansen, J. K. and Nicholls, J. G. (1973). Conductance changes, an electrogenic pump and the hyperpolarization of leech neurones following impulses. *J. Physiol.* **229**, 635-655.
Johansen, J. and Kleinhaus, A. L. (1986). Differential sensitivity of tetrodotoxin of nociceptive neurons in 4 species of leeches. *J. Neurosci.* **6**, 3499-3504.
Kaupp, U. B. and Seifert, R. (2001). Molecular diversity of pacemaker ion channels. *Annu. Rev. Physiol.* **63**, 235-257.
Klees, G., Hochstrate, P. and Dierkes, P. W. (2005). Sodium-dependent potassium channels in leech P neurons. *J. Membr. Biol.* **208**, 27-38.
Lucht, M. (1998). Elektrophysiologische und pharmakologische Charakterisierung von 5-Hydroxytryptamin-Rezeptoren und Second-messenger-Kaskaden bei identifizierten Neuronen des Blutegel-Nervensystems. PhD thesis, Heinrich-Heine-Universtität, Düsseldorf, Germany.
Ludwig, A., Budde, T., Stieber, J., Moosmang, S., Wahl, C., Holthoff, K., Langebartels, A., Wotjak, C., Munsch, T., Zong, X. et al. (2003). Absence epilepsy and sinus dysrhythmia in mice lacking the pacemaker channel HCN2. *EMBO J.* **22**, 216-224.
Lupica, C. R., Bell, J. A., Hoffman, A. F. and Watson, P. L. (2001). Contribution of the hyperpolarization-activated current (I_h) to membrane potential and GABA release in hippocampal interneurons. *J. Neurophysiol.* **86**, 261-268.
Macri, V., Proenza, C., Agranovich, E., Angoli, D. and Accili, E. A. (2002). Separable gating mechanisms in a mammalian pacemaker channel. *J. Biol. Chem.* **277**, 35939-35946.
Masino, M. A. and Calabrese, R. L. (2002). Period differences between segmental oscillators produce intersegmental phase differences in the leech heartbeat timing network. *J. Neurophysiol.* **87**, 1603-1615.
McCormick, D. A. and Pape, H. C. (1990a). Properties of a hyperpolarization-activated cation current and its role in rhythmic oscillation in thalamic relay neurones. *J. Physiol.* **431**, 291-318.
McCormick, D. A. and Pape, H. C. (1990b). Noradrenergic and serotonergic modulation of a hyperpolarization-activated cation current in thalamic relay neurones. *J. Physiol.* **431**, 319-342.
Meuth, S. G., Kanyshkova, T., Meuth, P., Landgraf, P., Munsch, T., Ludwig, A., Hofmann, F., Pape, H. C. and Budde, T. (2006). Membrane resting potential of thalamocortical relay neurons is shaped by the interaction among TASK3 and HCN2 channels. *J. Neurophysiol.* **96**, 1517-1529.
Mistrík, P., Pfeifer, A. and Biel, M. (2006). The enhancement of HCN channel instantaneous current facilitated by slow deactivation is regulated by intracellular chloride concentration. *Pflügers Arch.* **452**, 718-727.
Nicholls, J. (1987). The search for connections. In *Studies of Regeneration in the Nervous System of a Leech*, Magnes Lecture Series, Vol. 2, p. 25. Sunderland, MA: Sinauer Associates.
Pape, H. C. (1996). Queer current and pacemaker: the hyperpolarization-activated cation current in neurons. *Annu. Rev. Physiol.* **58**, 299-327.
Pape, H. C. and McCormick, D. A. (1989). Noradrenaline and serotonin selectively modulate thalamic burst firing by enhancing a hyperpolarization-activated cation current. *Nature* **340**, 715-718.
Pirtle, T. J., Willingham, K. and Satterlie, R. A. (2010). A hyperpolarization-activated inward current alters swim frequency of the pteropod mollusk *Clione limacina*. *Comp. Biochem. Physiol. A Mol. Integr. Physiol.* **157**, 319-327.
Proenza, C., Angoli, D., Agranovich, E., Macri, V. and Accili, E. A. (2002). Pacemaker channels produce an instantaneous current. *J. Biol. Chem.* **277**, 5101-5109.
Santoro, B., Liu, D. T., Yao, H., Bartsch, D., Kandel, E. R., Siegelbaum, S. A. and Tibbs, G. R. (1998). Identification of a gene encoding a hyperpolarization-activated pacemaker channel of brain. *Cell* **93**, 717-729.
Schlue, W. R. (1991). Effects of ouabain on intracellular ion activities of sensory neurons of the leech central nervous system. *J. Neurophysiol.* **65**, 736-746.
Schlue, W. R. and Deitmer, J. W. (1980). Extracellular potassium in neuropile and nerve cell body region of the leech central nervous system. *J. Exp Biol.* **87**, 23-43.
Schlue, W. R. and Deitmer, J. W. (1984). Potassium distribution and membrane potential of sensory neurons in the leech nervous system. *J. Neurophysiol.* **51**, 689-704.
Scuri, R., Mozzachiodi, R. and Brunelli, M. (2002). Activity-dependent increase of the AHP amplitude in T sensory neurons of the leech. *J. Neurophysiol.* **88**, 2490-2500.
Shin, K. S., Rothberg, B. S. and Yellen, G. (2001). Blocker state dependence and trapping in hyperpolarization-activated cation channels: evidence for an intracellular activation gate. *J. Gen. Physiol.* **117**, 91-101.
Siddall, M. E., Trontelj, P., Utevsky, S. Y., Nkamany, M. and Macdonald, K. S. (2007). Diverse molecular data demonstrate that commercially available medicinal leeches are not Hirudo medicinalis. *Proc. R. Soc. Lond B* **274**, 1481-1487.
Tobin, A. E. and Calabrese, R. L. (2005). Myomodulin increases I_h and inhibits the Na/K pump to modulate bursting in leech heart interneurons. *J. Neurophysiol.* **94**, 3938-3950.
Wollmuth, L. P. and Hille, B. (1992). Ionic selectivity of I_h channels of rod photoreceptors in tiger salamanders. *J. Gen. Physiol.* **100**, 749-765.
Wuttke, W. A. and Berry, M. S. (1992). Modulation of inwardly rectifying Na^+-K^+ channels by serotonin and cyclic nucleotides in salivary gland cells of the leech, *Haementeria*. *J. Membr. Biol.* **127**, 57-68.